arXiv:1302.2445v1 [cond-mat.quant-gas] 11 Feb 2013

Half-knot in the spinor condensates

Yong-Kai Liu and Shi-Jie Yang*
Department of Physics, Beijing Normal University, Beijing 100875, China

We present an exact solution to the stationary coupled nonlinear Gross-Pitaevskii equations which govern the motion of the spinor Bose-Einstein condensates. The solitonic solution is a twisted half-skyrmion in the three-dimension (3D) space. By making a map from and the Cartesian coordinates to the toroidal coordinates, we demonstrate it is a linked half-unknot with a fractional Hopf charge.

PACS numbers: 03.75.Mn, 03.75.Lm, 67.85.Fg

Topological objects appear in a variety of branches of physics from the liquid-crystal colloids[1], the classical field theory[2, 3], and the nonlinear optics[4, 5], to the condensed matter physics[6, 7] and the modern universe theory[8]. In the dilute atomic gas, quantized vortices and skyrmions have been widely studied and experimentally observed. In particular, the spinor Bose-Einstein condensation (BEC) whose spin direction can change dynamically has provided an ideal pilot to model and explore the rich family of topological excitations[9, 10].

The Hamiltonian of the spinor BEC has the $SO(3) \times U(1)$ symmetry. In contrast to ^4He superfluid where only the gauge symmetry is broken, the dilute atomic spinor BEC can also break the spin-rotational symmetry. A large amount of theoretical works has been carried out to study the nontrivial topological structures such as the fractional vortices, the skyrmions, the monopoles and the knots as well[11–17]. It is known that two kinds of spin textures, the Anderson-Thoulouse skyrmion and Mermin-Ho skyrmion, exist in 2D multi-component BECs. In 3D spinor BECs, monopoles, 3D skyrmions, as well as knots are theoretically predicted and numerically simulated.

According to the homotopy theory, the topological excitations are classified by the broken symmetry of the corresponding ground states[9, 10, 18]. They are characterized by the topological invariants. In the antiferromagnetic spinor BEC, the order parameter manifold is $M = S^2 \times U(1)/Z_2$. Here $U(1)$ denotes the manifold of the superfluid phase ϕ and S^2 is a two-dimensional sphere. The homotopy groups yield $\pi_n(M) \cong Z$ ($n = 1, 2, 3$). Singular line defects (vortices) and point defects (monopoles) are determined by the first and the second homotopy classes, $\pi_1(M)$ and $\pi_2(M)$, respectively[13,14]. The monopoles are sometimes called singular Skyrmions. The nontrivial third homotopy class $\pi_3(M)$ implies topological objects of knots. The corresponding topological invariant is called the Hopf charge which counts the number of times the 2D sphere covered by the 3D sphere.

The mean-field order parameter of the spinor BEC is governed by the coupled Gross-Pitaevskii equations (GPE). We present the exact solitonic solutions to the stationary GPEs for the $F = 1$ BEC in a uniform magnetic field. To our knowledge, this is the first analytical result to the coupled nonlinear equations in the 3D systems. Previous works are mainly in lower-dimensional space or/and by means of numerical simulations, in which the rich possibility of intriguing topological structures are often elusive[23]. Attempts for seeking analytical solutions to the coupled GPEs are usually frustrated by two obstacles: one is the nonlinear density-density interactions; the other is the nonlinear spin-spin interactions. We propose a method to decouple the equations by reassembling the spatial dimensions and the hyperfine states in the nonlinear density-density interactions. The complexity of the spin-spin couplings are surpassed by demanding that the hyperfine states satisfy $\psi_{-1} = -\psi_1^*$ and $\psi_0^* = \psi_0$, which yield the average of the spin-polarization $|\mathbf{F}| \equiv 0$. This vanishing spin-polarization state is most easily realizable in the antiferromagnetic BECs. The solitonic solution represents a twisted half-skyrmion in the three-dimension (3D) space and is demonstrated to be a linked half-unknot with a fractional Hopf charge.

The mean-field Hamiltonian reads,

$$H = \int d\mathbf{r} \sum_{m=0,\pm1} \psi_m^* [-\frac{\hbar^2}{2M}\nabla^2 - pm + qm^2 + V(\mathbf{r})]\psi_m + \frac{1}{2}\int d\mathbf{r}[c_0\rho^2 + c_2\mathbf{F}^2], \tag{1}$$

where the terms associated to p and q represent the linear and the quadratic Zeeman effects, respectively. $\rho(\mathbf{r}) = \sum_m |\psi_m(\mathbf{r})|^2$ is the total density of the condensate. The spin-polarization vector $\mathbf{F} = \sum_m \psi_m^* \hat{\mathbf{f}}_{mn}\psi_n/\rho$, with $\hat{\mathbf{f}}$ the spin matrices. The nonlinear coupling constants $c_0 = (g_0+2g_2)/3$ and $c_2 = (g_2-g_0)/3$, where g_F relating to the s-wave scattering length of the total spin-F channel as $g_F = 4\pi\hbar^2 a_F/M$. By choosing the units of $\hbar = M = 1$, the stationary GPEs in a uniform external field ($V(\mathbf{r}) = 0$) are written as

$$
\begin{aligned}
\mu\psi_1 &= [-\frac{1}{2}\nabla^2 - p + q + (c_0+c_2)(|\psi_1|^2+|\psi_0|^2) + (c_0-c_2)|\psi_{-1}|^2]\psi_1 + c_2\psi_0^2\psi_{-1}^*,\\
\mu\psi_0 &= [-\frac{1}{2}\nabla^2 + (c_0+c_2)(|\psi_1|^2+|\psi_{-1}|^2) + c_0|\psi_0|^2]\psi_0 + 2c_2\psi_0^*\psi_1\psi_{-1},\\
\mu\psi_{-1} &= [-\frac{1}{2}\nabla^2 + p + q + (c_0+c_2)(|\psi_-1|^2+|\psi_0|^2) + (c_0-c_2)|\psi_{-1}|^2]\psi_{-1} + c_2\psi_0^2\psi_1^*.
\end{aligned}
\tag{2}
$$

The 3D solitonic form of solutions is constructed as

$$
\Psi = \begin{pmatrix} -\frac{1}{\sqrt{2}}[\tanh(kx)\mathrm{sech}(ky) - i\mathrm{sech}(kx)\tanh(ky)]e^{-ik_z z} \\ \mathrm{sech}(kx)\mathrm{sech}(ky) \\ \frac{1}{\sqrt{2}}[\tanh(kx)\mathrm{sech}(ky) + i\mathrm{sech}(kx)\tanh(ky)]e^{ik_z z} \end{pmatrix}
\tag{3}
$$

where the periodic boundary condition in the z-direction requires $k_z = 2n\pi/L_z$ with n the number of modes. For simplicity, we have chosen $k_x = k_y \equiv k$. The total density of the condensate $\rho(\mathbf{r}) = \mathrm{sech}^2(kx) + \mathrm{sech}^2(ky)$ is uniform in the z-direction, which endues the Eqs.(2) be decoupled and the variables be separable according to the dimensions. This solution has solitonic form in the $x-y$ plane. The parameter relations are straightforwardly obtained by substituting the state (3) into the Eqs.(2) as $c_0 = -k^2$, $p = 0$, $q = -\frac{1}{2}k^2$, and $\mu = -k^2$. We note that the quadratic Zeeman energy plays the role of balancing the chemical difference between the hyperfine states.

The 3D order parameter can be rewritten as $\Psi(\mathbf{r}) = \sqrt{\rho(\mathbf{r})}\chi(\mathbf{r})$, where the $\chi(\mathbf{r})$ is a normalized spinor, $\chi^\dagger(\mathbf{r})\chi(\mathbf{r}) = 1$. Instead of the vanishing spin-polarization, we consider a real unit vector $\mathbf{d} = (d_x, d_y, d_z)^{\mathrm{T}}$, by which the spinor $\chi(\mathbf{r})$ is represented as[28, 29]

$$
\chi(\mathbf{r}) = \begin{pmatrix} \frac{-d_x + i d_y}{\sqrt{2}} \\ d_z \\ \frac{d_x + i d_y}{\sqrt{2}} \end{pmatrix}.
\tag{4}
$$

The $\mathbf{d}(\mathbf{r})$ vector is then given by

$$
\mathbf{d}(\mathbf{r}) = \frac{1}{\sqrt{\rho(\mathbf{r})}} \begin{pmatrix} \tanh(kx)\mathrm{sech}(ky)\cos(k_z z) - \mathrm{sech}(kx)\tanh(ky)\sin(k_z z) \\ \tanh(kx)\mathrm{sech}(ky)\sin(k_z z) + \mathrm{sech}(kx)\tanh(ky)\cos(k_z z) \\ \mathrm{sech}(kx)\mathrm{sech}(ky) \end{pmatrix}.
\tag{5}
$$

In quantum magnetism, $\mathbf{d}$ is also called the Néel vector which corresponds to the staggered magnetization of the antiferromagnetic state. Since $|\mathbf{d}| = 1$ and $\mathbf{d}_z > 0$ everywhere, it forms the surface of a semi-sphere in the order parameter manifold which is denoted as $S^2_{1/2}$. Here the subscript 1/2 indicates *half* of a sphere.

To reveal the topological structure of this state, we first examine the 2D situation which is fulfilled by simply setting $z = 0$ in the state (3). Figure 1(a) and (b) display the density distributions of the hyperfine states ψ_1 (or ψ_{-1}) and ψ_0, respectively. It shows that the hyperfine state ψ_1 (ψ_{-1}) forms a line-shape soliton, whereas ψ_0 forms a 2D point-shape soliton. The phase distribution of the ψ_1 (ψ_{-1}) in Fig.1(c) reveals a vortex (anti-vortex) at the center, where the ψ_0 component resides in. Therefore, the spinor BEC forms a coreless solitonic vortex. Fig.1(d) displays the spherical harmonic representation of the spinor condensate density which is expressed by $|\Psi(\mathbf{r}, \theta_{\mathrm{s}}, \phi_{\mathrm{s}})|^2 = |\sum_{m=0,\pm1}\psi_m(\mathbf{r})Y_{1m}(\theta_{\mathrm{s}}, \phi_{\mathrm{s}})|^2$, where $(\theta_{\mathrm{s}}, \phi_{\mathrm{s}})$ are the coordinates in the spin-space[9]. It exhibits a semi-hedgehog structure. We demonstrate this structure is a half-skyrmion as follows.

In 2D geometry, the vector $\mathbf{d}(\mathbf{r}) = \frac{1}{\sqrt{\rho(\mathbf{r})}}(\tanh(kx)\mathrm{sech}(ky), \mathrm{sech}(kx)\tanh(ky), \mathrm{sech}(kx)\mathrm{sech}(ky))^{\mathrm{T}}$ still represents the surface of a semi-sphere. The vectorial distribution of the $\mathbf{d}$ field is shown in Fig.2(a). The vector points upward at the center and gradually twists in the 2D plane at large distance. This texture represents a half-skyrmion which covers exactly half a sphere[30]. It is also called a Mermin-Ho Skyrmion or merlon which has been studied in the condensed matter physics such as the quantum Hall effects[19] and high temperature superconductivity[20]. It has also been created in the superfluid ^3He-A in a rotating cylinder[21, 22] and in

---

*Corresponding author: yangshijie@tsinghua.org.cn

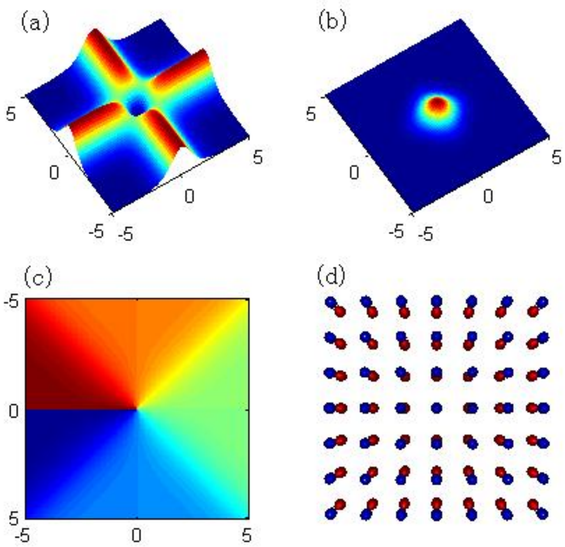

FIG. 1: (Color online) The 2D density distribution of the state (3) for (a) ψ_1 (or ψ_{-1}) and (b) ψ_0. (c) The phase distribution for ψ_{-1}. (d) The spherical harmonics representation of the spinor density.

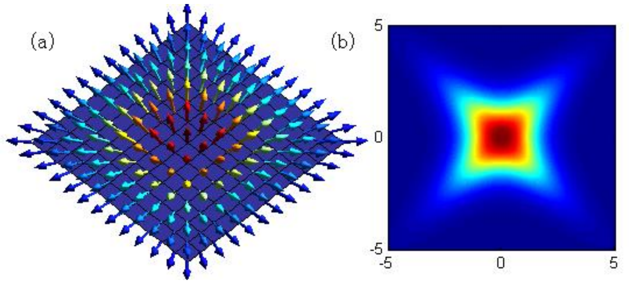

FIG. 2: (Color online) (a) The 2D texture of the **d** field. (b) The topological charge density $q(\mathbf{r})$. The total topological charge is $Q = 1/2$.

dilute atomic BEC by adiabatic deformation of the magnetic trap[11]. Fig.2(b) shows the topological charge density $q(\mathbf{r}) = \frac{1}{4\pi}\mathbf{d}\cdot(\partial_x\mathbf{d}\times\partial_y\mathbf{d})$, which characterizes the geometric distribution of the spin texture[28]. The total charge or the Pontryagian index $Q_{\mathrm{P}} = \int q(\mathbf{r})d\mathbf{r} = +1/2$ is a topological invariant[23, 24]. This is the reason why it is called a half-skyrmion. The anti-half-skyrmion solution with $Q_{\mathrm{P}} = -1/2$ can be obtained by simply taking the complex conjugacy of the state (3).

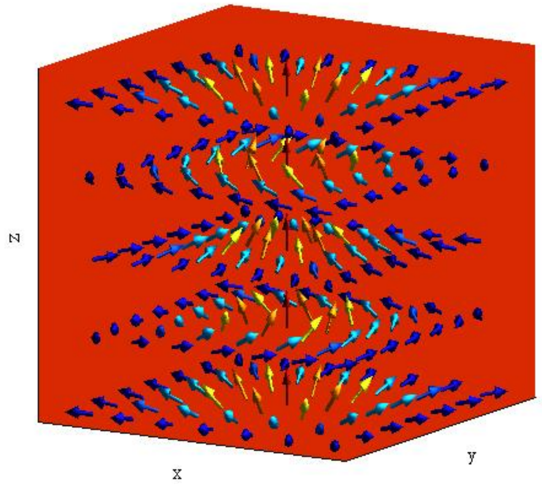

FIG. 3: (Color online) The 3D texture of the **d** field.

Now we further explore the 3D topological structure of the state (3). The periodic boundary condition in the z-direction implies that it essentially forms a twisted vortex ring. Figure 3 display the vectorial distribution of the $\mathbf{d}(\mathbf{r})$ vector in the 3D space. The vector points from upward at $z = 0$ to inplane at large distance while twists around the z-direction. The state that has a vanishing average spin-polarization implies it is locally degenerate [14]. The order parameter is invariant under an arbitrary rotation about $\mathbf{d}$, *i.e.*, $\exp[-i\mathbf{d}\cdot\hat{\mathbf{f}}\phi]\Psi = \Psi$, where ϕ is the rotation angle. The manifold of the unit **d** vector in the 3D space is similar to that in the 2D space. Since $\chi(\mathbf{r})$ is independent of any particular direction, it represents a mapping from a compactified 3D domain $(\mathbf{r})$ into a 2D semi-sphere in the order parameter space $R^3 \sim S^3 \to S^2_{1/2}$. The preimage of a point on the target $S^2_{1/2}$ corresponds to a closed loop in S^3. It can be characterized by a topological invariant called the Hopf charge, in integral formula which counts the number of times the two-sphere S^2 is covered by the three-sphere S^3.

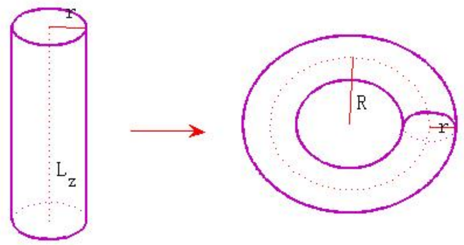

FIG. 4: (Color online) Schematic description of the mapping (6) from a cylinder to a torus. The symmetric axis of the cylinder is mapped as the core of the torus.

In order to get a more intuitive view of the topological structure, we make a mapping from the Cartesian coordinates to the toroidal coordinates by

$$\begin{pmatrix} x \\ y \\ z \end{pmatrix} \to \begin{pmatrix} \tilde{x} \\ \tilde{y} \\ \tilde{z} \end{pmatrix} = \begin{pmatrix} (x+R)\cos(z/R) \\ (x+R)\sin(z/R) \\ y \end{pmatrix}, \quad (6)$$

where $R = L_z/2\pi$ defines the size of the torus. This mapping transforms a cylinder with periodic boundary condition into a torus, as schematically shown in Fig.4. $|\tilde{\mathbf{r}}| = R$ indicates the position of the toroidal core. In terms of vector $\mathbf{d}$ it twists n-times around the core before joining the ends, implying it is a twisted vortex ring. Vortex rings have been studied experimentally in superfluid liquid helium [8, 9] and in Bose-Einstein condensates [10]. Numerical simulations have revealed that superfluid turbulence contains linked vortex lines [11]. Since we have the surface of a semi-sphere instead of a full sphere in the order parameter manifold, there are two types of distinct vortex rings: one is a twisted tube-ring; the other is a twisted Mobius strip, depending on the choice of the points on the $S^2_{1/2}$. Figure 5 schematically shows the two distinct mappings for the twisted tube ($d_z = 0.98$) and the twisted Mobius strip ($d_x = -0.98$). The color on the tube represents for the value of $\arctan(d_y/d_x)$ while on the Mobius strip the value of $\arctan(d_y/d_z)$. It helps to recognize the twisting feature of the tube or the strip. We mention that the color on the semi-sphere is just schematic and has no direct relevance to the color on the tube or the strip.

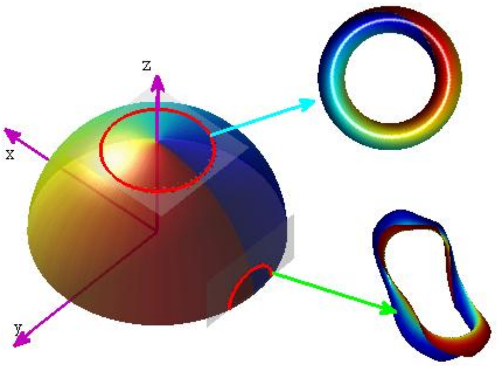

FIG. 5: (Color online) A loop (string) on the $S^2_{1/2}$ corresponds to a twisted tube (Mobius strip) in the real space. The color indicates the twisting number.

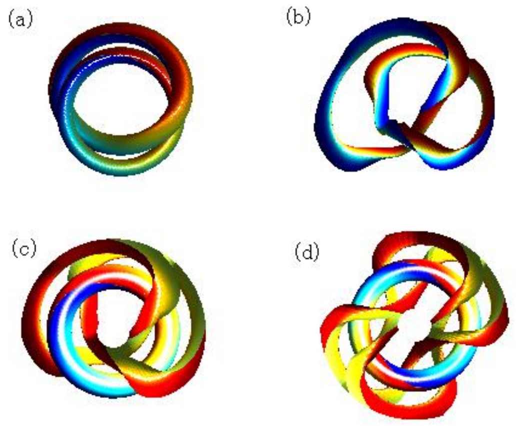

FIG. 6: (Color online) Two loops or two strings in the order parameter manifold correspond to two linked tubes (a) or two linked Mobius strips (b) in the real space. The twisting number equals to the linking number of the tubes or strips, *e.g.*, (c) and (d) One tube and two Mobius strips for $n = 1$ and $n = 2$, respectively.

In knot theory this twisted vortex ring defines an topological unknot, the simplest knot-like structure[2, 6]. The knot can be characterized by the Hopf charge which is defined by[7]

$$Q_{\mathrm{H}} = \frac{1}{4\pi}\int d^3\mathbf{r}\varepsilon_{ijk}\mathcal{F}_{ij}\mathcal{A}_k, \quad (7)$$

where $\mathcal{F}_{ij} = \partial_i\mathcal{A}_j - \partial_j\mathcal{A}_i = \mathbf{d}\cdot(\partial_i\mathbf{d}\times\partial_j\mathbf{d})$ is the strength of the gauge field and the vector $\mathbf{A}(\mathbf{r})$ defines a connection in the order parameter space. If the $\mathbf{d}$ field has Hopf charge Q_{H}, the tube or strip twists Q_{H} times. Furthermore, two loops corresponding to the preimages of any two distinct points on the target $S^2_{1/2}$ will be linked Q_{H} times. It is directly calculated that the state (3) has a fractional Hopf charge of $Q_{\mathrm{H}} = n/2$, where the factor $1/2$ comes from the semi-sphere instead of the full-sphere. Hence we call it the half-knot so as to differentiate it from the usual integral number of Hopf charge.

The topological structures are shown in Fig.6. Fig.6(a) is two linked twisted tubes which corresponds to two closed contours on the $S^2_{1/2}$ while Fig.6(b) is two linked Mobius strips which corresponds to two open strings for $d_x = 0.98$ and $d_y = 0.98$, respectively. Fig.6(c) and (d) are examples for three linked loops for $n = 1$ and $n = 2$, respectively. The linking number is equal to the twisting number of the tubes or strips.

In summary, we have constructed an exact solution to the coupled nonlinear GPEs in the 3D space. We revealed that it represents a solitonic knot with a half-integer topological charge. Our method may provide a clue to analytically solve other coupled nonlinear equations. Some relevant works will be published elsewhere.

This work is supported by the funds from the Ministry of Science and Technology of China under Grant No. 2012CB821403.

[1] G.E. Volovik and V.P. Mineev, Sov. Phys. JETP 45(6), 1186-1196 (1977); D. J. Thouless, Topological Quantum Numbers in Nonrelativistic Physics (World Scientific, Singapore, 1988).
[2] L. Faddeev and A. J. Niemi, Nature 387, 58C61 (1997).
[3] R. A. Battye and P. M. Sutcliffe, Phys. Rev. Lett. 81, 4798 (1998).
[4] W. T. M. Irvine and D. Bouwmeester, Nat. Phys. 4, 716-720 (2008).
[5] M. R. Dennis, R. P. King, B. Jack, K. OHolleran, and M. J. Padgett, Nat. Phys. 6, 118-121 (2010).
[6] E. Babaev, L. D. Faddeev, and A. J. Niemi, Phys. Rev. B 65, 100512 (2002).
[7] Y. Kawaguchi, M. Nitta, and M. Ueda, Phys. Rev. Lett. 100, 180403 (2008).
[8] A. Vilenkin and E. P. S. Shellard, Cosmic Strings and Other Topological Defects (Cambridge University Press, Cambridge, England, 1994).
[9] M. Ueda and Y. Kawaguchi, arXiv:1001.2072v3 (2012)(unpublished).
[10] Y. Kawaguchi, M. Kobayashi, M. Nitta, and M. Ueda, Prog. Theor. Phys. Suppl. 186, 455-462 (2010).
[11] A. E. Leanhardt, Y. Shin, D. Kielpinski, D. E. Pritchard, and W. Ketterle, Phys. Rev. Lett. 90, 140403 (2003).
[12] L. E. Sadler, J. M. Higbie, S. R. Leslie, M. Vengalattore, and D. M. Stamper-Kurn, Nature 443, 312 (2006).
[13] J.-P. Martikainen, A. Collin, and K.-A. Suominen, Phys. Rev. Lett. 88, 090404 (2002).
[14] V. Pietilä and M. Möttönen, Phys. Rev. Lett. 103, 030401 (2009).
[15] N . D. Mermin and T. L. Ho, Phys. Rev. Lett. 36, 594 (1976).
[16] T. Mizushima, K. Machida, and T. Kita, Phys. Rev. Lett. 89, 030401 (2002).
[17] P. W. Anderson and G. Toulouse, Phys. Rev. Lett. 38, 508 (1977).
[18] H. Mäkelä, J. Phys. A: Math. Gen. 39, 7423-7439 (2006).
[19] L. Brey, H. A. Fertig, R. Cote, and A. H. MacDonald, Phys. Rev. B 54, 16888-16902 (1996).
[20] T. Morinari, Phys. Rev. B 72, 104502 (2005).
[21] V. M. H. Ruutu, J. Kopu, M. Krusius, U. Parts, B. Placais, E. V. Thuneberg, and W. Xu, Phys. Rev. Lett. 79, 5058-5061 (1997).
[22] R. Ishiguro, O. Ishikawa, M. Yamashita, Y. Sasaki, K. Fukuda, M. Kubota, H. Ishimoto, R. E. Packard, T. Takagi, T. Ohmi, and T. Mizusaki, Phys. Rev. Lett. 93, 125301 (2004).
[23] S.-J. Yang, Q.-S. Wu, S.-N. Zhang, and S. Feng, Phys. Rev. A 77, 033621 (2008).
[24] S.-W. Su, I.-K. Liu, Y.-C. Tsai, W. M. Liu, and S.-C. Gou, Phys. Rev. A 86 023601 (2012).
[25] C.-F. Liu, and W. M. Liu, Phys. Rev. A 86, 033602 (2012).
[26] S. Kobayashi, Y. Kawaguchi, M. Nitta, and M. Ueda, Phys. Rev. A 86, 023612 (2012).
[27] K. Moon, H. Mori, K. Yang, S. M. Girvin, A. H. MacDonald, L. Zheng, D. Yoshioka, and S. C. Zhang, Phys. Rev. B 51, 5138-5170 (1995).
[28] J.-Y. Choi, W. J. Kwon, and Y.-I. Shin, Phys. Rev. Lett. 108, 035301 (2012).
[29] H. Zhai, W. Q. Chen, Z. Xu, and L. Chang, Phys. Rev. A 68, 043602 (2003).
[30] A. Saxena, R. Dandoloff, Phys. Rev. B 66, 104414 (2002).